

# Quantitative structure-activity relationship study and directed synthesis of Thieno[2,3-*d*]pyrimidine-2,4-diones as monocarboxylate transporter 1 inhibitors

O. T. Devinyak · Mikh. V. Slivka · Mar. V. Slivka ·  
V. M. Vais · V. G. Lendel

Received: 8 March 2010 / Accepted: 8 July 2011 / Published online: 23 July 2011  
© Springer Science+Business Media, LLC 2011

**Abstract** The aim of any quantitative structure-activity relationship (QSAR) study is not only to reveal relationships between structure of molecules and their biological activity, but also to explain it within the bounds of theoretical conceptions and to use the obtained model for prediction of properties of new compounds. That provides possibility to execute directed synthesis of new compounds with required biological activities. Monocarboxylate transporter 1 (MCT1) is one of the targets in a search for new immune response modulating and antitumor agents. In the present study, QSAR model for MCT1 binding affinity is developed. Decisive influence of relative negative partial charge, solvation energy, and radius of gyration on MCT1 inhibition has been detected. Theoretical explanation of the obtained model is given, and biological activity prediction for a series of *N*-vinyl derivatives of thieno[2,3-*d*]pyrimidine-2,4-dione is made. Directed synthesis of three leading compounds has been executed according to prediction results.

**Keywords** QSAR · Thieno[2,3-*d*]pyrimidine-2,4-dione · Monocarboxylate transporter 1 inhibitor · *N*-vinyl derivatives · In silico screening · Directed synthesis

## Introduction

Activation of T-cells following antigen challenge is an important component of the immune response. However, excessive activation of T-cells can lead to plenty of autoimmune diseases and a reaction of transplant rejection. Immunosuppressive agents, which are used to prevent the rejection of transplanted organs or tissues and to treat autoimmune diseases or diseases that are most likely of autoimmune origin (e.g., rheumatoid arthritis, multiple sclerosis, myasthenia gravis, systemic lupus erythematosus, Crohn's disease, pemphigus, ulcerative colitis, etc.), have numerous side-effects and risks (Berchtold and Seitz, 1996; Niethammer *et al.*, 1999; Rifai *et al.*, 2006). Therefore, the search for new compounds with immunosuppressive activity is important and actual.

The monocarboxylate transporters are a family of proteins which transport lactate and other small monocarboxylates. It was proved that the monocarboxylate transporter 1 (MCT1) expression grows rapidly after T-lymphocyte activation in order to eliminate lactate from the cell, the quantity of which grows as a result of increased glycolytic rate. Inhibition of lactate efflux by potent blockade of lactate transport results in an accumulation of lactate within the cell and feedback inhibition of glycolysis. This suppression of cellular metabolism, without being cytotoxic, results in an inability of T-lymphocytes to sustain the rapid rate of cell division, that takes place during the early immune response to antigen appearance. Thus, blockade of MCT1 is a new mechanism of immunosuppression distinct from current therapies (Murray *et al.*, 2005).

In addition, it has been reported that the blocking of lactate transport to tumor cells is one of the reliable methods to fight tumor growth. Experimental studies

O. T. Devinyak (✉) · V. M. Vais  
Department of Pharmaceutical Disciplines, Uzhgorod National  
University, Narodna sq., 1, Uzhgorod 88000, Ukraine  
e-mail: o.devinyak@gmail.com

Mikh. V. Slivka · Mar. V. Slivka · V. G. Lendel  
Department of Organic Chemistry, Uzhgorod National  
University, O. Fedince Str., 53/1, Uzhgorod 88000, Ukraine

O. T. Devinyak  
Transcarpathian State University, Zankovecka Str., 89a,  
Uzhgorod 88000, Ukraine

promise MCT1 inhibition to be a new, efficient anticancer treatment both by itself and combined with radiotherapy (Sonveaux *et al.*, 2008).

Thieno[2,3-*d*]pyrimidine-2,4-dione derivatives are characterized by several biological activities. Alpha-1 adrenoreceptor antagonists (Russell *et al.*, 1988), luteinizing hormone-releasing hormone receptor antagonists (Sasaki *et al.*, 2003), gonadotropin-releasing hormone receptor antagonists (Betz *et al.*, 2008), melanocortin receptor agonists or antagonists (Sharma and Shi, 2005), and also MCT1 inhibitors (Guile *et al.*, 2006) have been discovered in this class of compounds.

The purpose of current study is to reveal the dependence of MCT1 inhibiting rate on molecular structure and to execute directed synthesis of new thieno[2,3-*d*]pyrimidine-2,4-dione derivatives with high MCT1 inhibiting activity.

## Results and discussion

### Data sets

The comparativeness and homogeneity of experimental data is an important precondition for perfect QSAR model development because the values of the same activity for same compounds vary due to the experimental conditions and methods. Thus, MCT1 inhibition coefficients ( $K_i$ ) used for QSAR modeling were obtained during careful data analysis from literature (Guile *et al.*, 2006). The analysis shows that out of 37 compounds with obtained  $K_i$  there were only 22 compounds evaluated in the same assay (filter binding assay). So only these compounds and their experimental data were used for model development and validation. The complete set of compounds was divided into corresponding training and test sets based on MCT1 binding affinity. Since the  $K_i$  varied by orders of magnitude, to guarantee the linear distribution of the dependent variable, the  $K_i$  values were transformed to logarithmic values [ $\text{p}K_i = -\log(1/K_i)$ ], listed in Table 1. Before descriptors calculations, molecular geometries were pre-optimized by molecular mechanics calculations using the MMFF94x force field as implemented in MOE, 2007 .09 (Chemical Computing Group Inc).

### QSAR model building

About 250 descriptors used as independent variables in QSAR modeling were calculated using MOE software. Then, all data processing was performed in MATLAB 7.7 (The MathWorks, Inc). The whole data was divided into a training (16 compounds) and a test sets (6 compounds). This proportion was selected as the compromise between 1/3 of data as recommended (Gramatica, 2007) and the

apprehensiveness to get too small training set. In an ideal case, all the compounds have to be uniformly split into two samples both in the descriptors' space and by their activity. In the present study, it was decided to split data set using  $\text{p}K_i$  values. For this purpose, compounds were sorted by the activity in the ascending order, and every fourth compound (starting from the first) was classified as test one. The uniformity of test and training sets in the descriptors' space was checked using principal component analysis (PCA), particularly by the projection of data into first two principal components plane. The result (Fig. 1) shows satisfactory compounds distribution by their descriptor values.

A stepwise regression technique was used in order to construct the model of MCT1 binding affinity. Stepwise regression is a systematic method for adding and removing terms from a multilinear model based on their statistical significance in a regression (Draper and Smith, 1998). Using default regression parameters (maximum  $p$  value for a term to be added = 0.05, minimum  $p$  value for a term to be removed = 0.10), only three descriptors were selected:

- $\text{PEOE\_RPC}$ — relative negative partial charge;
- $E_{\text{sol}}$  solvation energy;
- $\text{rgyr}$  radius of gyration.

The calculated values for selected descriptors are listed in Table 2.

In order to reveal intercorrelations of independent variables and to discover the role of each descriptor in the resulting model, a pair-wise correlation analysis was performed, and correlation matrix of selected descriptors and  $\text{p}K_i$  was calculated (Table 3). Multi-collinearity between the above mentioned three descriptors was tested by calculating their variance inflation factors ( $VIF$ ) (Studenmund, 2006). If  $VIF$  equals to 1.0—no intercorrelation exists for each variable, and if it is larger than 5.0—that means that the related model is unstable and a recheck is necessary. The corresponding  $VIF$  values of selected descriptors are shown in Table 4. As can be seen from this table, all the variables have  $VIF$  values less than 2.0. Both the results show the absence of significant intercorrelations between selected descriptors, indicating that obtained model's coefficients have obvious statistic significance (Allen, 1997).

Statistical parameters of QSAR model are the following:  $N = 16$ ;  $R^2 = 0.878$ ;  $p < 10^{-5}$ ;  $F = 28.71$ ;  $Q_{\text{LOO}}^2 = 0.8105$ ;  $Q_{\text{ext}}^2 = 0.7946$ ,  $\text{RMSE} = 0.2236$ ;  $\text{RMSEP}_{\text{LOO}} = 0.2789$ ;  $\text{RMSEP}_{\text{ext}} = 0.3342$ , where  $N$  is the number of compounds used,  $R^2$  is the squared correlation coefficient,  $p$  is the significance level of the model,  $F$  is the Fisher ratio,  $Q_{\text{LOO}}^2$  and  $Q_{\text{ext}}^2$  are the squared correlation coefficients for Leave-One-Out and external validations, respectively,  $\text{RMSE}$  is the Root Mean Squared Error of the model (also known as standard deviation of regression,  $S$ ),  $\text{RMSEP}_{\text{LOO}}$

**Table 1** Molecular structures with the corresponding observed and predicted MCT1 inhibition activity

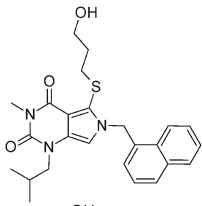
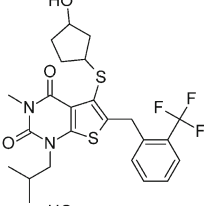
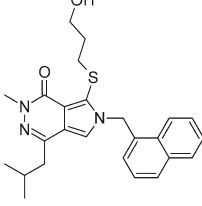
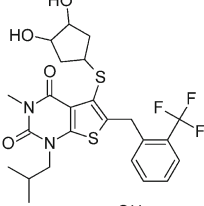
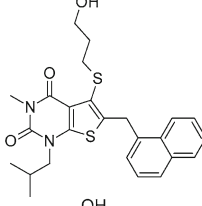
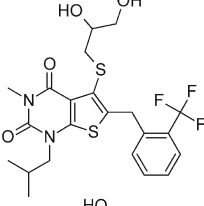
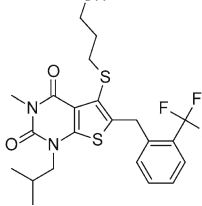
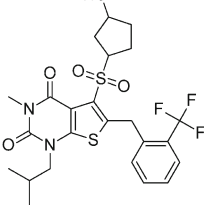
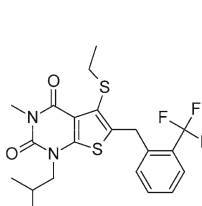
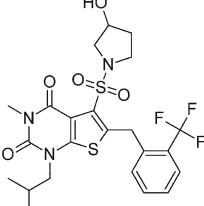
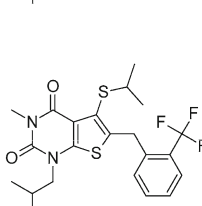
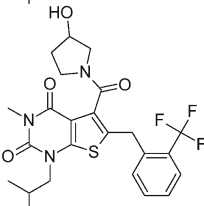
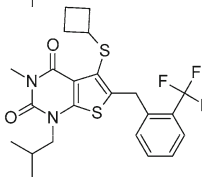
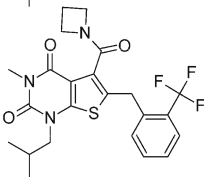
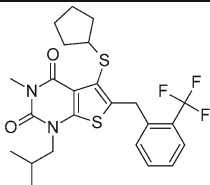
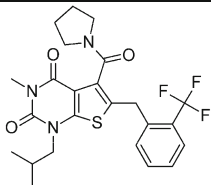
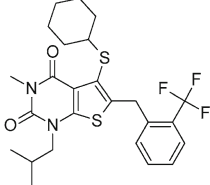
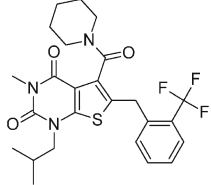
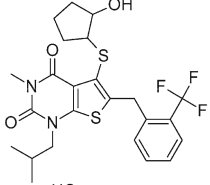
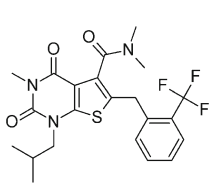
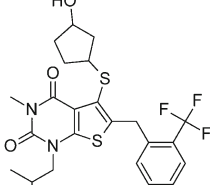
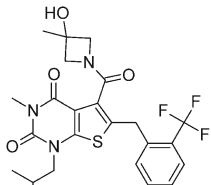
No	Molecular Structure	pK <sub>i</sub> observed	pK <sub>i</sub> calculated	No	Molecular Structure	pK <sub>i</sub> observed	pK <sub>i</sub> calculated
<b>1</b>		9.48	9.63	<b>12*</b>		9.38	9.16
<b>2</b>		10.00	9.95	<b>13</b>		9.17	9.21
<b>3*</b>		9.55	10.08	<b>14</b>		8.19	8.28
<b>4</b>		9.46	9.59	<b>15</b>		7.92	8.30
<b>5</b>		8.22	8.18	<b>16</b>		8.96	8.56
<b>6</b>		8.66	8.37	<b>17</b>		8.31	8.55
<b>7</b>		7.89	8.19	<b>18</b>		8.04	7.82

Table 1 continued

<b>8</b>		8.49	8.54	<b>19*</b>		8.26	8.00
<b>9</b>		8.22	8.29	<b>20*</b>		8.06	8.03
<b>10*</b>		8.57	8.94	<b>21*</b>		7.43	7.80
<b>11</b>		9.54	9.15	<b>22</b>		8.46	8.39

Compounds labeled with “\*” are the test set; and other compounds are the training set

and  $RMSEP_{ext}$  are Root Mean Squared Errors of Prediction in Leave-One-Out and external validation procedures, respectively.

The obtained statistical parameters and model validation results indicate its high quality and predictive power. A plot of predicted  $pK_i$  versus experimental  $pK_i$  values for both the training and test sets is shown in Fig. 2.

The agreement observed between the predicted and experimental values confirmed the efficiency of this QSAR model. In order to find outliers, the plot of the residuals (predicted  $pK_i$  – experimental  $pK_i$ ) versus experimental  $pK_i$  (Fig. 3) was studied. Considering the 3 standard deviation limit line ( $3S$ ) for spotting outliers, all the data were retained in the model.

Stepwise regression method gives the ability to find a minimum number of variables necessary to build an adequate model, but there is no guarantee that the obtained model is globally optimal. Thus, the genetic algorithm as more powerful global search heuristics was used as implemented in QSAR\_BENCH software (Konovalov *et al.*, 2007). In particular, the variable selection procedure was carried out by RMSEP minimization in Monte-Carlo

cross-validation using genetic algorithm (GA-MCVS) with iterations number  $N = 100\,000$ , validation set size  $n_v = 7$ , and number of variables  $n = 3$  (Konovalov *et al.*, 2008). The data filtering was executed; and constant, repeated, and intercorrelated (with  $|r| > 0.9$ ) descriptors were discarded preliminarily. The results have shown that the minimum root mean squared error of prediction ( $RMSEP = 0.3607$ ) is represented by the previously obtained descriptor set. It means that the obtained model has a great probability to be globally optimal.

#### QSAR model interpretation

As it is indicated by model, normalized coefficients shown in Table 4 and correlation coefficients between descriptors and  $pK_i$  (Table 3), the highest significance for MCT1 inhibition activity belongs to relative negative partial charge ( $PEOE_{RPC-}$ ). It is calculated as the smallest negative partial charge  $q_i$  divided by the sum of the negative partial charges  $q_i$ . And atomic partial charges in a molecule are obtained using Partial Equalization of Orbital Electronegativities (PEOE) method (Gasteiger and Marsili, 1980).

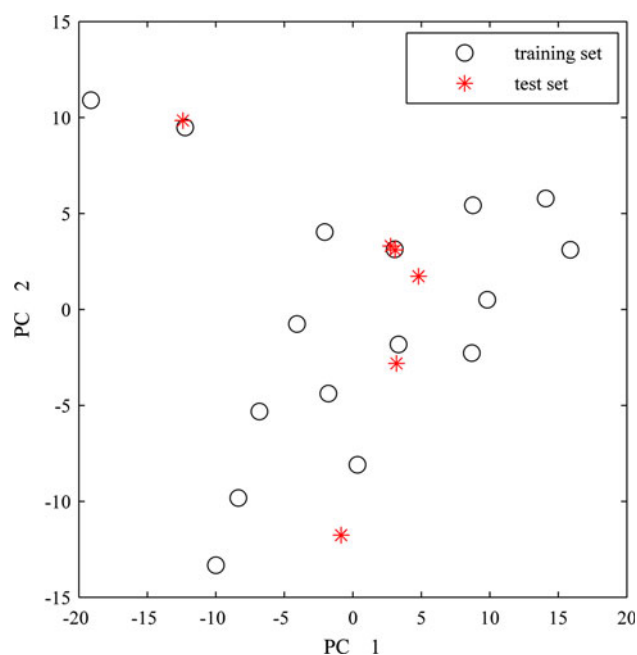


**Fig. 1** Projection of the compounds into first two principal components plane (PC 1 and PC 2 describe 34.2 and 19.7% of total variance, respectively)

**Table 2** Calculated descriptor values for chemical structures

Compound	<i>PEOE_RPC</i> –	<i>E<sub>sol</sub></i>	<i>rgyr</i>
1	0.1563	3.3014	4.3210
2	0.1835	–16.4083	4.2096
3*	0.1696	–6.2025	4.4744
4	0.1508	8.1924	4.3448
5	0.1336	1.8911	3.8918
6	0.1312	6.9452	4.0009
7	0.1297	2.6764	3.9850
8	0.1268	9.3244	4.1868
9	0.1241	–7.7311	4.3740
10*	0.1446	–8.9567	4.3396
11	0.1467	–7.5846	4.4109
12*	0.1467	–7.2084	4.4112
13	0.1296	21.6715	4.3766
14	0.1316	–7.5933	4.1793
15	0.1364	–10.9105	4.1285
16	0.1282	1.8018	4.2967
17	0.1266	–0.9526	4.3732
18	0.1251	–4.7219	3.9626
19*	0.1229	–11.4607	4.2640
20*	0.1206	–10.8194	4.3337
21*	0.1279	–2.6092	3.8486
22	0.1244	3.1249	4.2520

Compounds labeled with “\*” are the test set; and other compounds are the training set

**Table 3** Correlation matrix of experimental  $pK_i$  values and molecular descriptors selected for MCT1 binding affinity model development

	$pK_i$ observed	<i>PEOE_RPC</i> –	<i>E<sub>sol</sub></i>	<i>rgyr</i>
$pK_i$ observed	1.000	0.782	0.057	0.537
<i>PEOE_RPC</i> –		1.000	–0.373	0.172
<i>E<sub>sol</sub></i>			1.000	0.079
<i>rgyr</i>				1.000

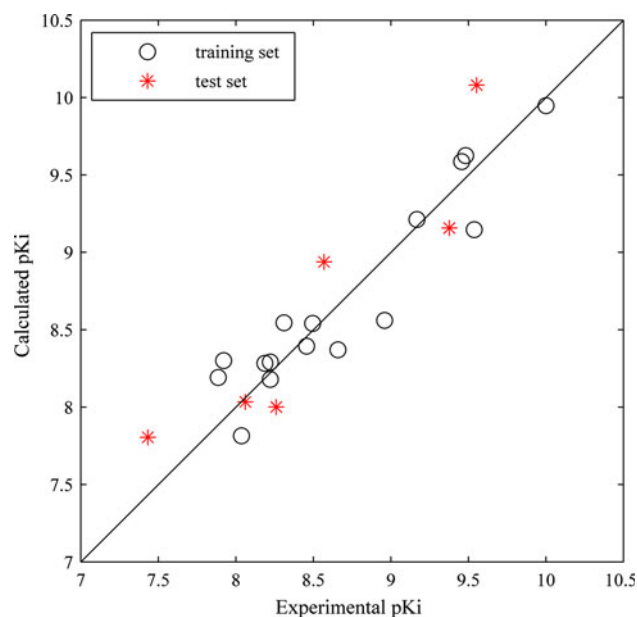
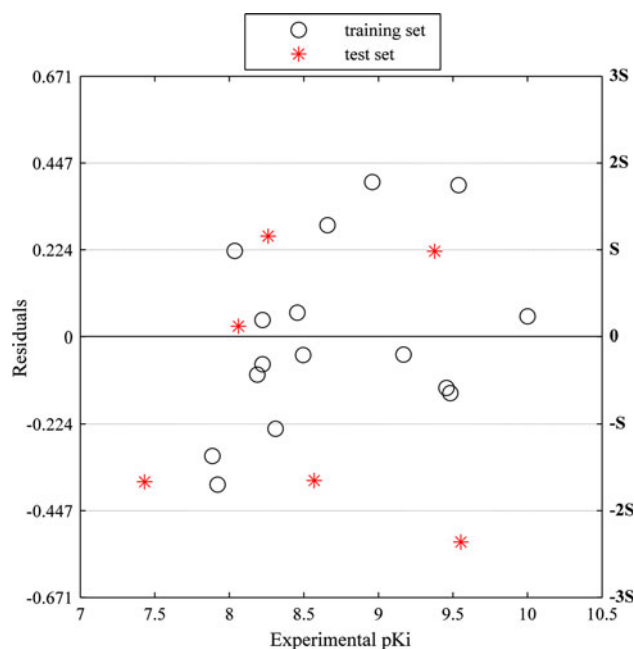
It means an important contribution of electrostatic interaction to MCT1 low molecular weight ligand binding. The highest *PEOE\_RPC*– values are represented by the compounds that contain an atom with considerable negative partial charge on it. This opinion is perfectly harmonized by the fact that natural MCT1 ligands are monocarboxylates— anions of short-chain organic acids (such as lactate, pyruvate, acetate, acetoacetate,  $\beta$ -hydroxybutyrate) (Halestrap and Price, 1999). Monocarboxylates contain negative charge delocalized over two carboxylate oxygen atoms.

As a result, MCT1 blockers have to be found among organic acids, and other compounds that can form anions. Nevertheless, it is known that ions with a localized charge exist in the solvated state in polar solvents (such as water and biological fluids). Therefore, solvent molecules coordinated to ligand become a barrier for ligand binding. Thus, the solvation energy barrier overcoming is a necessary precondition for the interaction. Just that very case is considered by the second descriptor—solvation energy *E<sub>sol</sub>*. Its positive coefficient value means that the  $pK_i$  increases when solvent coordination is more difficult, and solvation sphere removing is easier. Since, there is not even a minimal correlation between *E<sub>sol</sub>* and  $pK_i$  (Table 3), this descriptor does not define MCT1 affinity itself, but it is an important restrictive factor for *PEOE\_RPC*–. This is confirmed by the negative value of correlation coefficient between *PEOE\_RPC*– and *E<sub>sol</sub>*. Thereby, the results obtained in this study QSAR model once more confirms the impossibility to develop perfect models using approaches that discard so called insignificant (from the standpoint of a single-parameter correlation) descriptors (e.g., heuristic descriptor pre-selection procedure implemented in CODESSA PRO - University of Florida, 2005).

The third descriptor included in the model is the radius of gyration *rgyr*. Its positive coefficient value means that spatially branched molecules will show higher affinity to MCT1. According to the authors’ opinion, it can be the result of additional weak hydrogen and van der Waals bonds formation. This formation plays a key role in ligand emplacement near the active site of protein molecule in the moment of proton accepting by anion because of equilibrium proton exchange between anionic ligand and the positively charged amino acid.

**Table 4** Descriptors, coefficients, normalized coefficients, standard errors, *t* values, and variance inflation factors for the linear model

Physico-chemical meaning	Descriptors	Coefficient	Normalized coefficient	Standard error	<i>t</i> value	VIF
Intercept	Constant	−2.1411	−3.3483	1.6909	−1.266	
Relative negative partial charge	<i>PEOE_RPC</i> −	35.3745	0.8479	4.6509	7.6059	1.2193
Solvation energy	<i>E<sub>sol</sub></i>	0.0245	0.3448	0.0078	3.1294	1.1908
Radius of gyration	<i>rgyr</i>	1.425	0.3637	0.4066	3.5047	1.0563

**Fig. 2** Calculated versus experimental  $pK_i$  values for both the training and test sets. The diagonal in the plot is the  $y = x$  line**Fig. 3** Residuals versus experimental  $pK_i$  values for both training and test sets

### QSAR model application

In order to reveal leading compounds among potent MCT1 blockers, in silico screening of *N*-vinyl derivatives of thieno[2,3-*d*]pyrimidine-2,4-dione was carried out. The whole set of evaluated compounds is presented in Table 5.

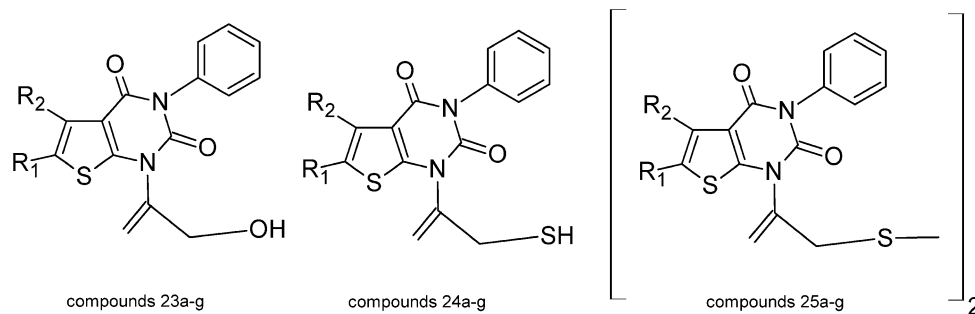
Deliberately reducing the molecular weight and complexity (compounds **23a–g** and **24a–g** in comparison with the compounds **1–22** used for model building and validation) an increase of *PEOE\_RPC*− values was achieved, but *rgyr* and *E<sub>sol</sub>* values decreased (Table 2 vs. Table 5). As a result of the model application, high  $pK_i$  values for a number of derivatives containing alcoholic hydroxyl (compounds **23a–g**, Table 5) were predicted. The predicted  $pK_i$  values for thiol derivatives (compounds **24a–g**) were lower. And for both the series of molecules, larger  $pK_i$  were observed for compounds with condensed cyclopentene or cyclohexene rings (**23f,g** and **24f,g**). Several dimers with considerably decreased *PEOE\_RPC*− simultaneously with the increased *rgyr* and *E<sub>sol</sub>* values (compounds **25a–g**) were also included to the set of screening compounds. This dimers have shown higher predicted MCT1 affinities

than the corresponding monomers (**24a–g**). But the anion formation from compounds **25a–g**, that may be essential for MCT1 binding, is possible only after former hydrolysis. So these compounds can be regarded only as prodrugs.

In modern drug discovery programs, compliance of molecular structures with drug likeness criteria has a high importance. Therefore, Lipinski's drug-like test (Lipinski *et al.*, 1997) and Oprea's lead-like test (Oprea, 2000) (both implemented in MOE) were conducted for the studied compounds. Results showed that molecular structures **23a–g** and **24a–g** meet all the criteria. Molecular structures **25a–g** failed both the drug-like and lead-like tests.

Since the compounds **23f** and **23g**, and **24f** and **24g** have the very close predicted  $pK_i$  values, in order to select leading compounds to synthesize, the following analysis was made. From the drug structure database *DrugBank* (<http://www.drugbank.ca>) the two samples of molecules containing, respectively, cyclopentene or cyclohexene ring as a substructure were received. So 115 structures with cyclohexene ring, and only 10 structures with cyclopentene ring were found. Since there is more than a tenfold



**Table 5** Selected descriptors and predicted  $pK_i$  values for analyzed compounds

Compound	$R_1$	$R_2$	$PEOE_{RPC}$	$E_{sol}$	$rgyr$	$pK_i$ (predicted)
<b>23a</b>	CH <sub>3</sub>	H	0.2005	−14.8547	3.4041	9.44
<b>23b</b>	CH <sub>3</sub>	CH <sub>3</sub>	0.1979	−13.2489	3.4415	9.44
<b>23c</b>	CH <sub>3</sub>	C <sub>2</sub> H <sub>5</sub>	0.1931	−13.7838	3.5130	9.36
<b>23d</b>	CH <sub>3</sub>	<i>n</i> -C <sub>3</sub> H <sub>7</sub>	0.1882	−9.7605	3.5775	9.37
<b>23e</b>	CH <sub>3</sub>	iso-C <sub>3</sub> H <sub>7</sub>	0.1890	−12.4710	3.5961	9.36
<b>23f</b>		(CH <sub>2</sub> ) <sub>3</sub>	0.1965	−12.7736	3.5247	9.51
<b>23g</b>		(CH <sub>2</sub> ) <sub>4</sub>	0.1913	−12.5710	3.6372	9.50
<b>24a</b>	CH <sub>3</sub>	H	0.1595	−12.8694	3.4455	8.09
<b>24b</b>	CH <sub>3</sub>	CH <sub>3</sub>	0.1572	−12.1241	3.4873	8.09
<b>24c</b>	CH <sub>3</sub>	C <sub>2</sub> H <sub>5</sub>	0.1529	−11.8150	3.5528	8.04
<b>24d</b>	CH <sub>3</sub>	<i>n</i> -C <sub>3</sub> H <sub>7</sub>	0.1485	−11.4918	3.6061	7.97
<b>24e</b>	CH <sub>3</sub>	iso-C <sub>3</sub> H <sub>7</sub>	0.1493	−12.5344	3.6415	8.02
<b>24f</b>		(CH <sub>2</sub> ) <sub>3</sub>	0.1559	−12.7663	3.5669	8.14
<b>24g</b>		(CH <sub>2</sub> ) <sub>4</sub>	0.1513	−12.6884	3.6773	8.14
<b>25a</b>	CH <sub>3</sub>	H	0.0839	−15.4518	5.2819	7.97
<b>25b</b>	CH <sub>3</sub>	CH <sub>3</sub>	0.0826	0.0983	5.2233	8.23
<b>25c</b>	CH <sub>3</sub>	C <sub>2</sub> H <sub>5</sub>	0.0803	−6.9993	5.8252	8.83
<b>25d</b>	CH <sub>3</sub>	<i>n</i> -C <sub>3</sub> H <sub>7</sub>	0.0779	−17.4794	5.9173	8.62
<b>25e</b>	CH <sub>3</sub>	iso-C <sub>3</sub> H <sub>7</sub>	0.0782	−15.2369	5.6233	8.27
<b>25f</b>		(CH <sub>2</sub> ) <sub>3</sub>	0.0819	6.0621	5.6502	8.96
<b>25g</b>		(CH <sub>2</sub> ) <sub>4</sub>	0.0794	−16.3663	5.8241	8.57

difference in the sizes of the received samples, it was decided to synthesize cyclohexene derivatives, specifically:

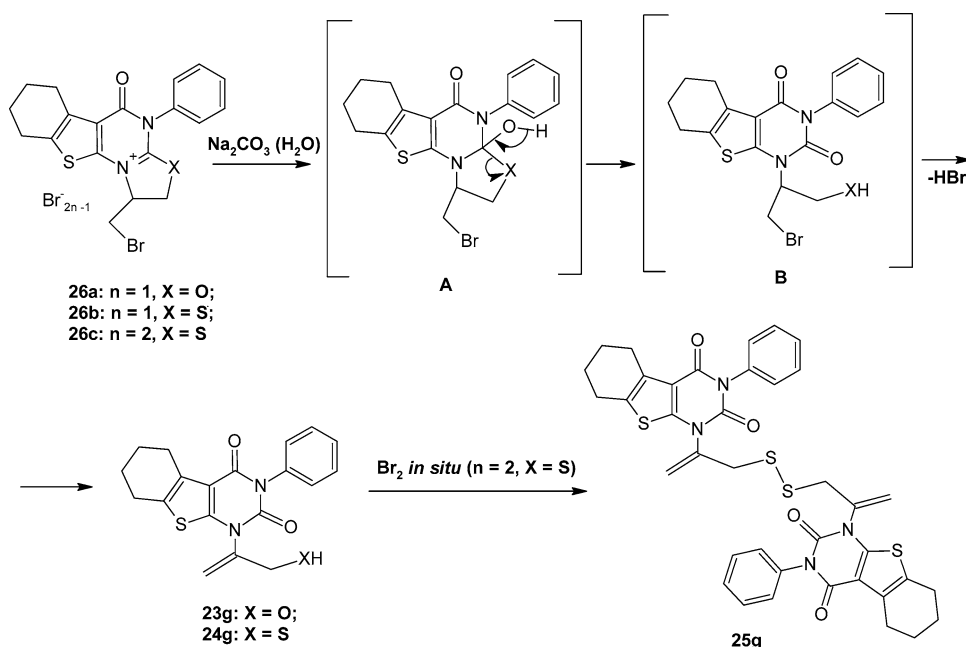
- Compound **23g**—as a leading compound with the highest predicted  $pK_i$  value;
- Compounds **24g** and **25g**—as model representatives of the series **24a–g** and **25a–g**, respectively.

## Chemistry

A convenient way to get vinyl functional derivatives of heterocycles by splitting oxazoline or thiazoline rings was chosen (Slivka *et al.*, 2008). Oxazolino(thiazolino-)thienopyrimidine salts **26a–c** were chosen as starting compounds. An active electrophilic center located at the “nodal” Carbone was used as the reaction center. The preparative methods of

splitting oxazolino(thiazolino-)thienopyrimidinium bromides **26a–c** were developed by varying synthesis conditions and the nature of nucleophilic reagent (Scheme 1).

Nucleophilic cleavage was carried out by the action of sodium carbonate. In the first phase, the attack of hydroxyl group on the “nodal” carbon of pyrimidine cycle is implemented with the next addition and pseudo-base (**A**) formation. Then the destruction of oxazolidine (thiazolidine) ring takes place with the intermediate (**B**) formation, and under the influence of strong nucleophile the elimination of hydrogen bromide follows. This leads to the formation of *N*-vinyl derivatives of thieno[2,3-*d*]pyrimidine-2,4-dione **23g** and **24g**. In the case of formation of *N*-thiovinyl derivatives from corresponding tribromides compound **25g** is received. This can be explained by the presence of free bromine molecules in the reaction atmosphere, acting as

**Scheme 1** Synthesis of selected compounds

oxidants of previously formed aliphatic mercapto groups. The overall reaction is shown in Scheme 1.

Known methods of synthesis from the corresponding allyl(thio-)ethers were used for the preparation of starting oxazolino(thiazolino-)thienopyrimidinium bromides **26a–c** (Khripak *et al.*, 2004).

## Conclusions

The study of quantitative relationship between molecular structure and monocarboxylate transporter 1 inhibition is carried out and QSAR model that can predict  $pK_i$  is obtained in present study. It is shown that the inhibition constant increases with increasing relative negative partial charge, solvation energy, and radius of gyration of molecules. Using obtained QSAR model, the activities of *N*-vinyl derivatives of thieno[2,3-*d*]pyrimidin-2,4-dione are predicted, and the leading compound is identified. The synthesis of the leading compound and two model representatives of the studied molecules is executed, and preparative methods of current synthesis are developed. Further investigations of the synthesized compounds in vitro and in vivo are necessary for QSAR model optimization and for optimization of the leading compound structure.

## Experimental section

### Statistical methods and model validation

The goodness of fit of the model was evaluated using the following statistical parameters: the squared correlation

coefficient ( $R^2$ ); the Root Mean Squared Error of the model (RMSE, also known as the standard deviation of regression  $S$ ); the significance of the model ( $p$ ); and the Fisher ratio value ( $F$ ).

The predictive stability and robustness of the model depends not only on model building approaches, but also on the quality of initial data. Therefore, in order to detect multicollinearity between the selected descriptors the variance inflation factors (VIF) were calculated as follows:  $VIF = 1/(1 - R^2)$ , where  $R^2$  is the correlation coefficient of multiple regression between one variable and the others in the model.

Validation procedure is the most important step in the development of reliable QSAR models. Obtained QSAR model was first verified by internal cross-validation by calculating the following parameters:  $Q_{LOO}^2$  (the squared correlation coefficient for Leave-One-Out cross-validation) and  $RMSEP_{LOO}$  (the Root Mean Squared Error of Prediction in Leave-One-Out validation). Using test set, the model was further checked by external validation by calculating parameters:  $Q_{ext}^2$  (the squared correlation coefficient for external validation) and  $RMSEP_{ext}$  (the Root Mean Squared Error of Prediction in external validation procedure).

### Chemistry

Melting points were determined in open capillaries on a Mel-Temp apparatus and are uncorrected. The purity of the compounds was confirmed by the thin-layer chromatography (TLC) performed on Sorbfil plates (Russia) at 27°C (silicagel, ethanol/diethyl ether/hexane 1:3:1). Spots were



detected by their absorption under UV light and by visualization using 0.05 mol I<sub>2</sub> in 10% HCl. IR spectra were recorded on an UR-20 spectrometer, as KBr pellets and wave numbers were given in cm<sup>-1</sup>.

<sup>1</sup>H NMR spectra were obtained using a Varian VXR-300 spectrometer (300 MHz) in DMSO-d<sub>6</sub>. Chemical shifts are reported in  $\delta$  values (ppm) relative to TMS  $\delta$  = 0 (<sup>1</sup>H), as internal standard. The microanalyses were performed on Perkin-Elmer 240C elemental analyzer.

The starting oxazolino(thiazolino-)thienopyrimidinium bromides **26a–c** were prepared according to the literature procedure (Khripak *et al.*, 2004).

*1-(3-hydroxyprop-1-en-2-yl)-3-phenyl-5,6,7,8-tetrahydrobenzo[b]thieno[2,3-d]pyrimidine-2,4(1H, 3H)-dione (23g)*

Monobromide **26a** (0.50 g, 1 mmol) was dissolved, when heated in 20 ml DMSO. To the stirred resulting mixture, a solution of sodium carbonate (0.53 g, 5 mmol) in 5 ml of water was added. The reaction mixture was stirred under heating at 70–80°C for 4 h, and then the hydrolysis product was precipitated by adding 100 ml of cooled water. Precipitate was filtered and washed by 50 ml of warm water acidified by 1 ml of acetate acid, and then was dissolved in ethanol heated to boiling. The mixture was cooled and formed during cooling precipitate was separated. The reaction product was participated from the filtrate by adding water and was crystallized from 50% ethanol–water solution. Yield: 69%. Colorless crystals; mp: 148–149°C; TLC:  $R_f$  = 0.78; <sup>1</sup>H NMR (300 MHz, DMSO-d<sub>6</sub>)  $\delta$ : 1.75 (m, 4H, 2CH<sub>2</sub>), 2.69 (m, 2H, CH<sub>2</sub>), 2.76 (m, 2H, CH<sub>2</sub>), 4.81–4.83 (m, 2H, CH<sub>2</sub>), 5.78 (s, 1H, =CH<sub>2</sub>), 6.14 (s, 1H, =CH<sub>2</sub>), 7.25–7.51 (m, 5H, C<sub>6</sub>H<sub>5</sub>) ppm; IR (KBr),  $\nu$ : 3400–3600 (O–H), 1680 (C=O) cm<sup>-1</sup>. Anal. Calcd. for C<sub>19</sub>H<sub>18</sub>N<sub>2</sub>O<sub>3</sub>S (354.423), %: C, 64.41; H, 5.08; N, 7.91; S, 9.04. Found, %: C, 64.11; H, 5.11; N, 7.97; S, 9.09.

*1-(3-mercaptoprop-1-en-2-yl)-3-phenyl-5,6,7,8-tetrahydrobenzo[b]thieno[2,3-d]pyrimidine-2,4(1H, 3H)-dione (24g)*

Monobromide **26b** (1.03 g, 2 mmol) was dissolved in 20 ml of heated DMSO. To the stirring and cooling resulting mixture, a solution of sodium carbonate (0.53 g, 5 mmol) in 5 ml of water was added dropwise. The reaction mixture was stirred at room temperature for 10 min, and then the hydrolysis product was precipitated by adding 100 ml of cooled water. Precipitate was filtered and washed by 50 ml of warm water acidified by 1 ml of acetate acid. The reaction product was crystallized from methanol. Yield: 54%. Light yellow crystals; mp: 123–125°C; TLC:  $R_f$  = 0.86; <sup>1</sup>H NMR (300 MHz, DMSO-

d<sub>6</sub>)  $\delta$ : 1.76 (m, 4H, 2CH<sub>2</sub>), 2.72 (m, 2H, CH<sub>2</sub>), 2.78 (m, 2H, CH<sub>2</sub>), 4.12 (s, 2H, CH<sub>2</sub>), 5.66 (s, 1H, =CH<sub>2</sub>), 5.92 (s, 1H, =CH<sub>2</sub>), 7.20–7.50 (m, 5H, C<sub>6</sub>H<sub>5</sub>) ppm; IR (KBr),  $\nu$ : 2480 (S–H), 1640 (C=O) cm<sup>-1</sup>. Anal. Calcd. for C<sub>19</sub>H<sub>18</sub>N<sub>2</sub>O<sub>2</sub>S<sub>2</sub> (370.488), %: C, 61.62; H, 4.86; N, 7.57; S, 17.30. Found, %: C, 61.51; H, 4.81; N, 7.62; S, 17.39.

*1,1'-(disulfanediyl)diprop-1-ene-3,2-diylbis(3-phenyl-5,6,7,8-tetrahydrobenzo[b]thieno[2,3-d]pyrimidine-2,4(1H, 3H)-dione) (25g)*

Tribromide **26c** (0.68 g, 1 mmol) was dissolved in 20 ml of heated DMSO. To the stirring and cooling resulting mixture, a solution of sodium carbonate (0.53 g, 5 mmol) in 5 ml of water was added dropwise. The reaction mixture was stirred at room temperature for 10 min, and then the hydrolysis product was precipitated by adding 100 ml of cooled water. Precipitate was filtered and washed by 50 ml of warm water acidified by 1 ml of acetate acid. The reaction product was crystallized from dioxane. Yield: 72%. Light yellow crystals; mp: 227–228°C; TLC:  $R_f$  = 0.64; <sup>1</sup>H NMR (300 MHz, DMSO-d<sub>6</sub>)  $\delta$ : 1.74 (m, 4H, 2CH<sub>2</sub>), 2.74 (m, 2H, CH<sub>2</sub>), 2.79 (m, 2H, CH<sub>2</sub>), 4.06 (s, 2H, CH<sub>2</sub>), 5.64 (s, 1H, =CH<sub>2</sub>), 5.90 (s, 1H, =CH<sub>2</sub>), 7.22–7.48 (m, 5H, C<sub>6</sub>H<sub>5</sub>) ppm; IR (KBr),  $\nu$ : 1640 (C=O) cm<sup>-1</sup>. Anal. Calcd. for C<sub>38</sub>H<sub>34</sub>O<sub>4</sub>N<sub>4</sub>S<sub>4</sub> (738.961), %: C, 61.79; H, 4.61; N, 7.59; S, 17.34. Found, %: C, 61.62; H, 4.51; N, 7.62; S, 17.42.

**Acknowledgments** The authors thank Transcarpathian Regional Charitable Foundation “Assistance to Students and Teachers of Medical Faculty Renaissance” for supporting this study.

## References

- Allen MP (1997) Understanding regression analysis. Plenum Press, New York, pp 176–180
- Berchtold P, Seitz M (1996) Immunosuppression—a tightrope walk between iatrogenic harm and therapy. *Schweiz Med Wochenschr* 38:1603–1609
- Betz SF, Zhu Y, Chen C, Struthers RS (2008) Non-peptide gonadotropin-releasing hormone receptor antagonists. *J Med Chem* 51(12):3331–3348
- Draper NR, Smith H (1998) Applied regression analysis. Wiley-Interscience, Hoboken, pp 307–312
- Gasteiger J, Marsili M (1980) Iterative partial equalization of orbital electronegativity—a rapid access to atomic charges. *Tetrahedron* 36:3219–3228
- Gramatica P (2007) Principles of QSAR models validation: internal and external. *QSAR Comb Sci* 26:694–701
- Guile SD, Bantick JR, Cheshire DR, Cooper ME, Davis AM, Donald DK, Evans R, Eyssade C, Ferguson DD, Hill S, Hutchinson R, Ingall AH, Kingston LP, Martin I, Martin BP, Mohammed RT, Murray C, Perry MWD, Reynolds RH, Thorne PV, Wilkinson DJ, Withnall J (2006) Potent blockers of the monocarboxylate transporter MCT1: novel immunomodulatory compounds. *Bioorg Med Chem Lett* 16:2260–2265

- Halestrap AP, Price NT (1999) The proton-linked monocarboxylate transporter (MCT) family: structure, function and regulation. *Biochem J* 343:281–299
- Khripak SM, Plesha MV, Slivka MV, Yakubets VI, Krivoviyaz AA (2004) Synthesis and reactivity of 1-bromomethyl-5-oxo-4-phenyl-1, 2, 4, 5, 6, 7, 8, 9-octahydrobenzo[4, 5]thieno[3, 2-e][1, 3]oxazolo[3, 2-a]-pyrimidin-11-ium bromides. *Zhurnal Organicheskoi Khimii* 40:1705–1706
- Konovalov DA, Coomans D, Deconinck E, Vander Heyden Y (2007) Benchmarking of QSAR models for blood-brain barrier permeation. *J Chem Inf Model* 47:1648–1656
- Konovalov DA, Sim N, Deconinck E, Vander Heyden Y, Coomans D (2008) Statistical Confidence for Variable Selection in QSAR models via Monte Carlo Cross-Validation. *J Chem Inf Model* 48:370–383
- Lipinski CA, Lombardo F, Dominy BW, Feeney PJ (1997) Experimental and computational approaches to estimate solubility and permeability in drug discovery and development settings. *Adv Drug Deliv Rev* 23:3–25
- Chemical Computing Group Inc. MOE 2007.09 (Molecular Operating Environment software). <http://www.chemcomp.com>
- Murray CM, Hutchinson R, Bantick JR, Belfield GP, Benjamin AD, Brazma D, Bundick RV, Cook ID, Craggs RI, Edwards S, Evans LR, Harrison R, Holness E, Jackson AP, Jackson CG, Kingston LP, Perry MW, Ross AR, Rugman PA, Sidhu SS, Sullivan M, Taylor-Fishwick DA, Walker PC, Whitehead YM, Wilkinson DJ, Wright A, Donald DK (2005) Monocarboxylate transporter MCT1 is a target for immunosuppression. *Nat Chem Biol* 1:371–376
- Niethammer D, Kümmerle-Deschner J, Dannecker GE (1999) Side-effects of long-term immunosuppression versus morbidity in autologous stem cell rescue: striking the balance. *Rheumatology* 38:747–750
- Oprea TI (2000) Property distribution of drug-related chemical databases. *J Comp Aided Mol Des* 14:251–264
- Rifai K, Kirchner GI, Bahr MJ, Cantz T, Rosenau J, Nashan B, Klempnauer JL, Manns MP, Strassburg CP (2006) A new side effect of immunosuppression: High incidence of hearing impairment after liver transplantation. *Liver Transpl* 12(3):411–415
- Russell RK, Press JB, Rampulla RA, McNally JJ, Falotico R, Keiser JA, Bright DA, Tobia A (1988) Thiophene systems. 9. Thienopyrimidinedione derivatives as potential antihypertensive agents. *J Med Chem* 31(9):1786–1793
- Sasaki S, Cho N, Nara Y, Harada M, Endo S, Suzuki N, Furuya S, Fujino M (2003) Discovery of a thieno[2, 3-d]pyrimidine-2, 4-dione bearing a p-methoxyureidophenyl moiety at the 6-position: a highly potent and orally bioavailable non-peptide antagonist for the human luteinizing hormone-releasing hormone receptor. *J Med Chem* 46(1):113–124
- Sharma SD, Shi Y (2005) Thieno[2,3-d]pyrimidine-2,4-dione melanocortin-specific compounds. US Patent 2005/0124636, 9 June 2005
- Slivka MV, Slivka MV, Usenko RM, Lendel VG (2008) Method of obtaining N-vinyl functional derivatives of 5,6-membered nitrogen-containing heterocycles. UA Patent 37721, 10 Dec 2008
- Sonveaux P, Végan F, Schroeder T, Wergin MC, Verrax J, Rabbani ZN, De Saedeleer CJ, Kennedy KM, Diepart C, Jordan BF, Kelley MJ, Gallez B, Wahl ML, Feron O, Dewhirst MW (2008) Targeting lactate-fueled respiration selectively kills hypoxic tumor cells in mice. *J Clin Invest* 118(12):3930–3942
- Studenmund AH (2006) Using econometrics: a practical guide, 5th edn. Pearson International Edition, New Delhi, pp 258–259
- The MathWorks, Inc. MATLAB (R2008b) (The Language of Technical Computing) Version 7.7.0.471. <http://www.mathworks.com>
- University of Florida (2005) CODESSA PRO user's manual. p 82. <http://www.codessa-pro.com>